IEEE Access
Multidisciplinary | Rapid Review | Open Access Journal

Received 2 March 2024, accepted 17 March 2024, date of publication 21 March 2024, date of current version 27 March 2024.

Digital Object Identifier 10.1109/ACCESS.2024.3380444

RESEARCH ARTICLE

Design of the Miniaturized and Thin Sliced-Type Beam Switching-Controlled Horn Antenna for D-Band

MING-AN CHUNG, (Senior Member, IEEE), CHIA-WEI LIN, AND ING-PENG MEIY
Department of Electronic Engineering, National Taipei University of Technology, Taipei 10608, Taiwan

Corresponding author: Ming-An Chung (mingannchung@mail.ntut.edu.tw)

This work was supported by the National Science and Technology Council, Taiwan, under Grant NSTC 112-2221-E-027-065.

ABSTRACT This paper proposes a design of a multilayer controlled beam horn antenna for the D-band. The multilayer design can achieve easy to control, low cost, and compact structure. The designed structure achieves the effect of a conventional horn antenna by stacking multiple layers and realizes the effect of beam switching by modifying the multi-layer plate structure. The widest bandwidth can be obtained when stacking 4 layers of boards, covering 24.7% (110-141GHz) of the bandwidth with a simulation gain of approximately 13.5dBi. By replacing the third plate structure, beam switching of ±30 degrees can be achieved, and the gain after beam switching can also reach 11.5 dBi.

INDEX TERMS Horn, antenna, D-band, beam switching, multi-layer.

I. INTRODUCTION

Due to the increasing demand for data capacity in communication systems, D-band has been selected as a potential communication band because of its low atmospheric absorption, very low latency, and large available bandwidth. Current applications for D-band [1], [2], [3], [4], [5], [6] communication include small base stations [7], short-range high-speed transmission [8], and automotive radar [9]. In the D-band, it is important to note the relatively high path loss and the dielectric loss generated by the substrate. These issues will be the most important challenges to overcome in designing D-band antennas.

To solve the losses generated by the path at millimeter wave frequencies, it is often necessary to design antennas with high directivity. In recent years, the way to improve the antenna gain is mostly through the array structure to achieve higher directivity, such as [3], [10], [11], [12], [13], and [14] are through the array structure to improve the radiation directivity. In [10], a slot array using corporate-feed is introduced to achieve a homogeneous feeding network through the slot waveguide, and metal pins are added to the radiation slot to increase the bandwidth. In [11], a high gain and high efficiency transmitting array antenna using low-temperature cofired ceramics (LTCC) technology with 360° phase coverage through a tunable substrate integrated waveguide is proposed. Therefore, it is clear that arrays are the most common way to increase gain, but it is important to consider that arrays require a complex feeding network, which can cause higher loss and make the design more difficult in the millimeter wave band.

In recent years, there are also discussions on such as Pérot cavity antenna [15], [16], reflector antenna [17], [18], [19], lens antenna [18], [20], [21], [22], [23], [24], [25], [26], [27], [28], and horn antenna [29], [30], [31], [32], [33], [34], [35], [36], [37], [38], [39], [40]. In [15], the phase shift feeder and the phase shift surface are designed using the LTCC technique and the holder is designed using the 3D printing technique. The designed results can achieve about 17.5dBi and 17.1dBi dual polarization gain. In [17], a quasi-parabolic reflector was proposed and the antenna was made beam-controlled by swapping the feed source. In [20], it is proposed to design the lens through three dielectric materials so that it increases the range of transmission and reception of the packaged antenna. In [21], a controlled, highly directional, and low scanning loss is achieved by the integration of two lenses. In [29], [31],

The associate editor coordinating the review of this manuscript and approving it for publication was Shah Nawaz Burokur.

[41], [42], [43], and [44], multilayer metal horn antennas are designed on PCB boards, and the metal structure of the horn is simulated by metal via. The results presented show a wide bandwidth and high antenna gain. In [32], a tapered horn structure is designed with packaging metal to improve the antenna performance. In [33], a substrate integrated waveguide (SIW) feed is used to excite and achieve a bandwidth of 129.5-156.5 GHz with good antenna gain by adding a horn antenna.

This paper proposes a multi-layer PCB with an integrated Horn antenna structure. Each layer of the PCB is designed through a progressive structure, and each layer uses Via as the metal wall to mimic a standard horn antenna. The Horn antenna is able to control the radiation phase shift through different substrate structures, and the performance of the proposed antenna structure in terms of radiation gain and phase switching is verified by actual measurements.

II. GUIDELINES FOR MANUSCRIPT PREPARATION

A. MULTILAYER HORN ANTENNA

This paper proposes a low-cost multilayer horn structure antenna, and the proposed antenna has a periodic structure. It has the high gain, broadband, and pronounced radiation directivity of a traditional horn antenna. To imitate the conductive wall of a conventional horn antenna, the metal wall is replaced by a periodic stepped ring via. In Fig. 1(a), the cross-section of the designed multilayer horn antenna is shown. The antenna feed end is fed by a WR-6.5 waveguide as the feed port, and the structure is made of a 4-layer Arlon Diclad 880 substrate (dielectric coefficient of 2.2, tangential loss of 0.0009, and substrate thickness of 0.508mm). Fig. 1(b) is an exploded view of the structure, and Fig. 1(c) is a top view of the antenna. The bottom layer is the ground plane connected to the WR-6.5 waveguide, and the whole structure is fixed by screws and locating pins.

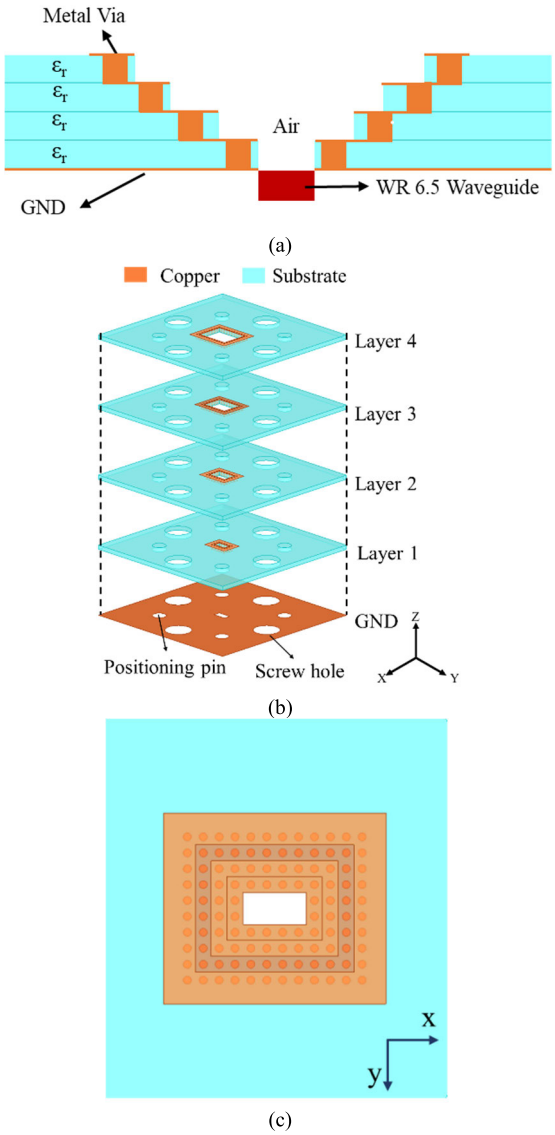

FIGURE 1. Structure of the multilayer horn antenna. (a) Cross-sectional view. (b) Exploded view. (c) Top view.

B. ANALYZING ANTENNA STRUCTURE

Fig. 2 shows the reflection coefficients and simulated gains of the basic structure for 3-, 4-, and 5-layers stacked to study the effect of different layer numbers on the antenna. As shown in Fig. 2(a) and (b), the reflection coefficient of the structure with 3 layers is about 110-135 GHz and the gain is about 8-10dBi at 110-150 GHz. The structure with 4 layers has a bandwidth of 120-145 GHz with a reflection coefficient below the −10dB standard, and the antenna gain is about 9-11dBi at110-150 GHz. When the number of stacked layers increases to the fifth layer, the reflection coefficient will be lower than −10 dB at 110-126 and 140- 148GHz, and the gain is about 10-13.5dBi at 110-150 GHz. The bandwidth of the 3-layers structure is 110-135 GHz, which is worse than the 4- and 5-layers structures in terms of gain performance. Although the 5-layers structure has the maximum antenna gain at 140-150 GHz, the bandwidth of the reflection coefficient does not reach the maximum bandwidth of the 4-layers structure. Therefore, a four-layer horn antenna architecture will be chosen as the base. In Fig. 3, the radiation patterns of the 3, 4, and 5-layers structures are shown. The yz-plane of Fig. 3(a) shows that at the overlapping 125GHz, the radiation gain of the 3-layer structure is about 7dBi at 0 degrees, and the maximum gain of the structure with 4 layers is about 10dBi, with more obvious directivity. The 5-layer structure shows the maximum radiation gain at plus or minus 30 degrees.

The xz-plane in Fig. 3(b) shows that the structure with 3 layers has an antenna gain of 8 dBi at 0 degrees, which is 2 dBi different from the 10 dBi of the structure with 4 layers. The five layers also shows the maximum radiation gain at plus or minus 30 degrees.

C. BEAM CONTROL DESIGN

In this section, beam direction control is performed by switching the structure of the 3rd layer substrate to achieve the result of beam transformation. The structure of the design

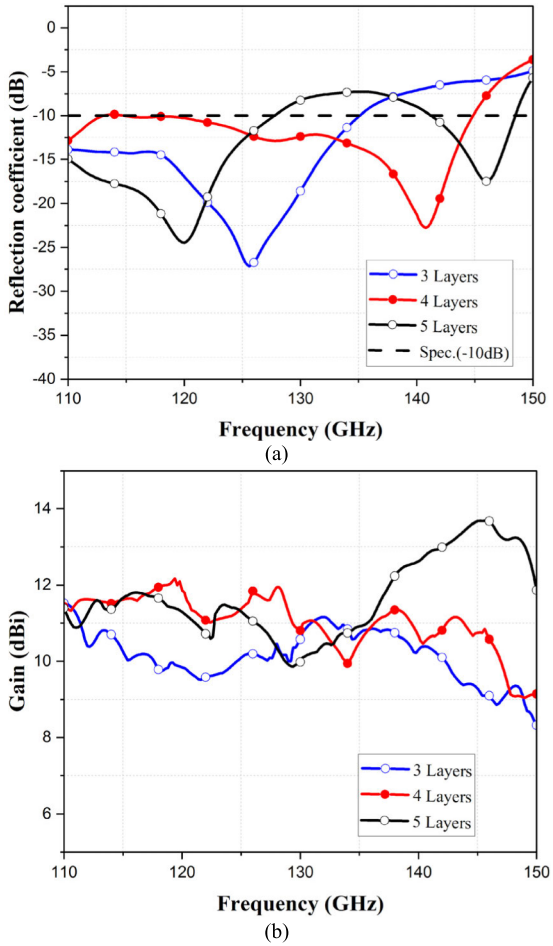

FIGURE 2. Analysis of the stacked horn structure. (a) Reflection coefficient. (b) Gain.

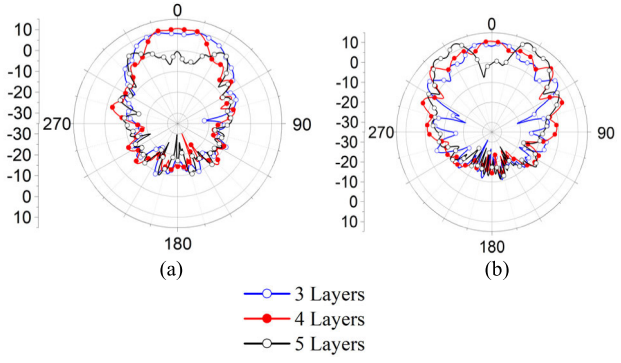

FIGURE 3. Radiation pattern for different stacking quantities. (a) yz-plane. (b) xz plane.

is shown in Fig. 4. Fig. 4(a) shows the detailed dimensions of the proposed multilayer horn antenna. In the third layer of the structure, two additional structures are designed to increase the via metal wall, and this structure adjusts the rectangular groove of length b_5 length to b_{r1}. Fig. 4(b) shows the cross-sectional view of the antenna. It can be seen in layer 3 of the structure along the via metal wall, respectively.

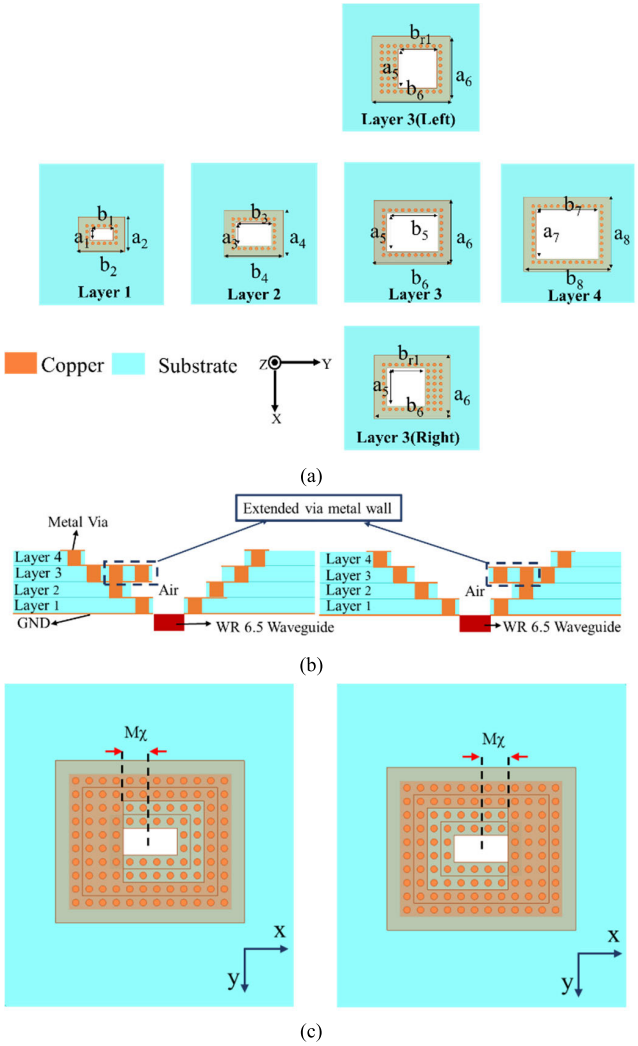

FIGURE 4. Detailed specifications of each multilayer horn antenna. (a) Dimensions (b) Cross-section (c) Top view. ($a_1 = 0.8$mm, $a_2 = 2.4$mm, $a_3 = 1.6$mm, $a_4 = 3.2$mm, $a_5 = 2.4$mm, $a_6 = 4.4$mm, $a_7 = 3.2$mm, $a_8 = 4.8$mm, $b_1 = 1.6$mm, $b_2 = 3.2$mm, $b_3 = 2.4$mm, $b_4 = 4$mm, $b_5 = 3.2$mm, $b_6 = 4.8$mm, $b_7 = 4$mm, $b_8 = 5.6$mm, and $b_{r1} = 2.4$mm.)

Fig. 4(c) shows the multilayer antenna extending in both directions of vias, where Mχ is used asthe distance from the metal wall to the center point along the extended via.

Since the multilayer structure is modified, the reflection coefficients of the original antenna structure and the fixed addition of via metal walls (M_x progressively shorter) towards the feed center are analyzed in Fig. 5. The bandwidth of the Mχ can be seen to cover 114.8-145GHz at the -10 dB reflectance coefficient standard at the original size of 1.6mm. When the Mχ is reduced to 0.8mm, the bandwidth covers 116.8-150 GHz. When the Mχ is reduced to 0mm, the bandwidth is shifted to a low frequency of 110-125.8 GHz.

Then discuss the beam change affected by increasing the via metal wall (M_x progressively shortened). Fig. 6 shows that when Mχ is at the original size of 1.6 mm, the radiation pattern in the yz-plane is concentrated at 0 degrees, and when Mχ is at 0.8 mm, the radiation pattern has a directional angle

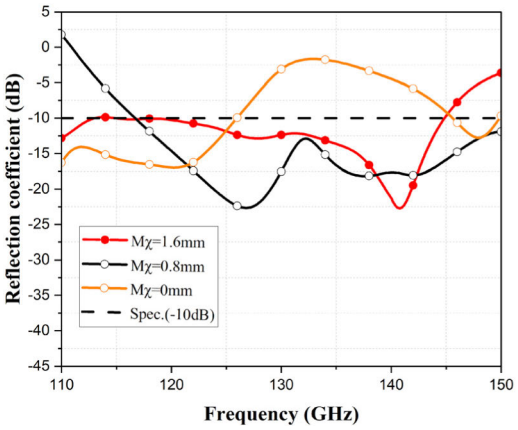

FIGURE 5. Reflection coefficient analysis of via parameter Mχ.

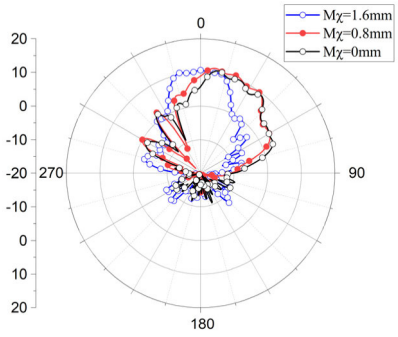

FIGURE 6. Radiation pattern of the parameter Mχ.

of 15 degrees. The radiation pattern of M_x at 0mm is similar to that of Mχ at 1.2 mm, with a phase shift of about 15 degrees.

III. MEASUREMENT RESULTS AND VALIDATION

The proposed multilayer horn antenna is fabricated on a low-cost PCB board as shown in Fig. 7. In Fig. 7(a) a physical photograph of all stacked layers is shown, and the antenna size is 20 mm × 20 mm. Fig. 7(b) shows the complete structure fixed by locating pins and screws, also shows the measurement environment.

A. MULTILAYER HORN ANTENNA MEASUREMENT RESULTS

The measured reflectance coefficients of the multi-layer horn antennas are in Fig. 8. The results show that the simulated and measured results are similar, but the overall measured bandwidths are toward the lower bandwidths, which are included in the 110-141 GHz. Fig. 9 shows the simulated and measured gain comparisons. The measured results show that the gain is about 13.5 dBi overall, with a maximum peak gain of 14 dBi at 135 GHz, and the simulated average gain is about 10 dBi at 110-150 GHz, while the maximum gain can reach 11.2 dBi. The actual gain increases by about 3.5dB when compared to the simulated result. The measured and simulated yz- and xz-plane radiation patterns are shown in Fig. 10. Due to

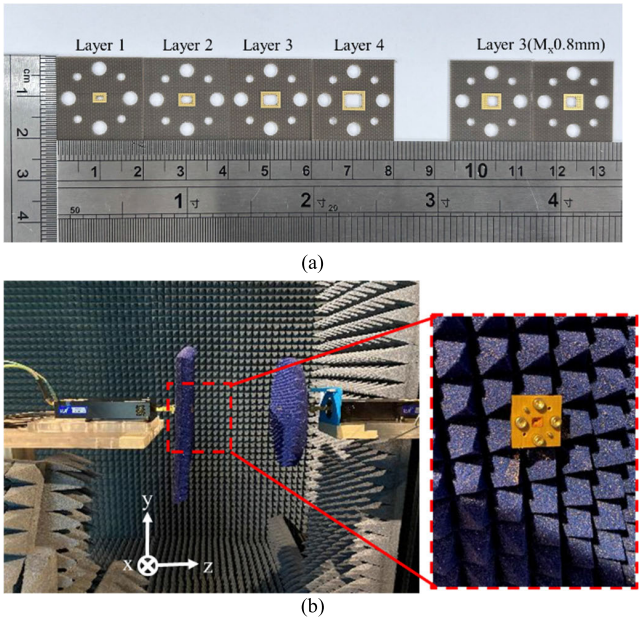

FIGURE 7. Fabricated multilayer horn antenna. (a) Dimensions. (b) Measurement environment.

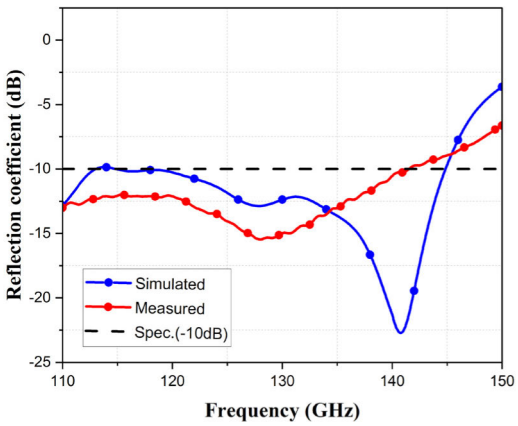

FIGURE 8. Results of the measurement of the reflection coefficient.

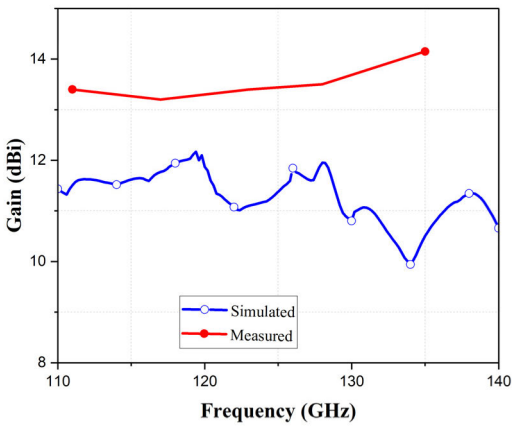

FIGURE 9. Simulated and measured gain.

the measurement environment, it is not possible to measure the radiation direction from90degrees to 270 degrees. The measured radiation pattern has the maximum radiation gain

TABLE 1. Comparison of horn antenna documents in similar frequency bands in recent years.

Ref.	Antenna Type	Layer	Size(mm^2)	Substrate	Height(mm)	Frequency (GHz)	Gain(dBi)	Beam Switching
Pro.	**Multilayer horn**	**4**	**20×20**	**DiClad 880**	**2.032**	**110-141 (23.2%)**	**13.5**	**Yes**
[29]	Multilayer horn	5	30×3.5	Rogers/ Duroid 6002	2.5	70-105 (40%)	9.5	No
[32]	Antenna-in-Package horn	12	28×16	Ferro A6	7.052	88-98 (10.7%)	12.3	No
[33]	Stainless-steel-based horn	1	5×5	Rogers 5880	6	129.5-156.5 (18.9%), 125.3-154.4 (20.7%)	7.26	No

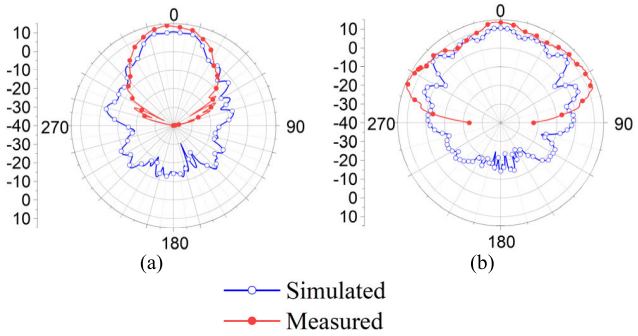

FIGURE 10. Measurements of (a) yz-plane and (b) xz-plane radiation patterns at 130 GHz.

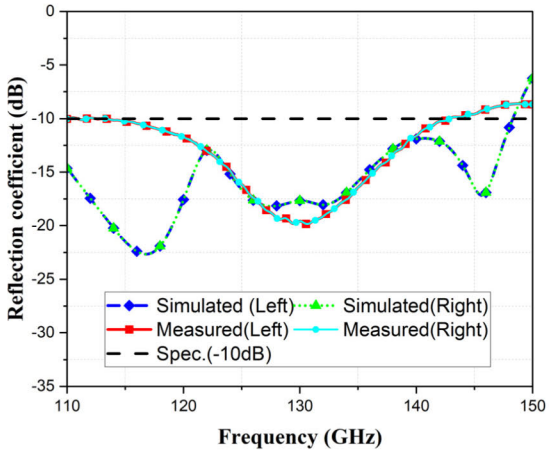

FIGURE 11. Comparison of the reflection coefficients of switched materials.

at 0 degree, which is the same as the simulated result. The trend is consistent in the yz plane, while the xz plane shows a wider radiation pattern.

B. MEASUREMENT AND SIMULATION OF DIFFERENT THIRD-LAYER MATERIALS

The reflection coefficients for switching materials are shown in Fig. 11. The measured bandwidth covers 111-142.8 GHz, which is reduced compared to the simulated reflectance

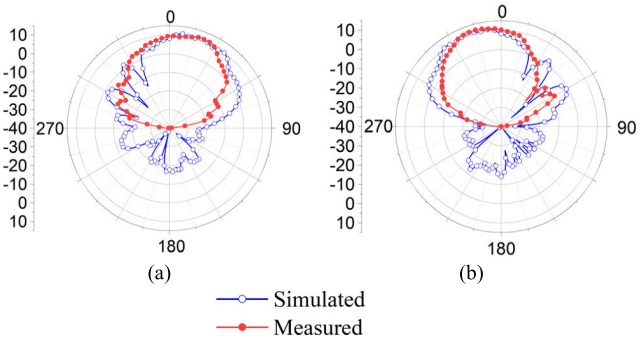

FIGURE 12. The xyz-plane radiation pattern at 130 GHz for the switched plate. (a) Right side and (b) left side.

coefficient of 107-148.8 GHz, and the actual measured reflectance coefficient is reduced by resonance at 118 and145.5 GHz. Fig. 12 shows the radiation pattern of the multilayer horn antenna and the replacement material. The radiation pattern of the basic multilayer horn antenna tends to be concentrated at 0 degrees and has a radiation gain of 10 dBi. The radiation pattern is kept at plus or minus 15 degrees of beam shift.

C. LITERATURE COMPARISON

In Table 1, a comparison of the designed multilayer horn antenna with recent literature on horn antennas in similar frequency bands will be presented here. The proposed antenna architecture has the thinnest structure thickness and a higher radiation gain compared to [29], [32], and [33], and has a wider operating bandwidth in terms of reflectance coefficient compared to the literature [32], [33]. The proposed antenna can control the direction of the beam by switching plates. The proposed design provides more flexibility than a fixed beam direction and offers high gain and a thinner structure thickness.

IV. CONCLUSION

In this paper, a controlled beam multilayer horn antenna design for D-band is designed. The designed multilayer horn

antenna shows a consistent reflectance coefficient bandwidth for both measurement and simulation in the substrate switching structure and achieves a reflectance coefficient bandwidth of 110-147.9 GHz (29.3%) with a peak gain of 11 dBi for measurement. The reflection coefficient after replacing multiple layers of substrates also maintains similar results to the measured results, covering an effective bandwidth of 113-142.8 GHz at −10 dB standard. The measured radiation pattern has a phase-switching ratio of plus or minus 30 degrees at 10 dBi radiation gain. It shows that the designed structure has good consistency and robustness. The proposed multilayer horn antenna design can meet the advantages of controllable beam phase, simple structure, and low cost, indicating that the antenna has good prospects for application in D-band communication systems.

REFERENCES

[1] C. Gu, S. Gao, V. Fusco, G. Gibbons, B. Sanz-Izquierdo, A. Standaert, P. Reynaert, W. Bösch, M. Gadringer, R. Xu, and X. Yang, "A D-band 3D-printed antenna," *IEEE Trans. THz Sci. Technol.*, vol. 10, no. 5, pp. 433–442, Sep. 2020.

[2] S. Erdogan, K. J. Moon, M. Kathaperumal, and M. Swaminathan, "D-band integrated and miniaturized quasi-yagi antenna array in glass interposer," *IEEE Trans. THz Sci. Technol.*, vol. 13, no. 3, pp. 270–279, May 2023.

[3] X. Wang, G. Xiao, L. Yang, H. Li, and Q. Xu, "Broadband D-band patch antenna array in wafer-level package based on BCB process," *IEEE Open J. Antennas Propag.*, vol. 3, pp. 1172–1179, 2022.

[4] M. de Kok, A. B. Smolders, and U. Johannsen, "A review of design and integration technologies for D-band antennas," *IEEE Open J. Antennas Propag.*, vol. 2, pp. 746–758, 2021.

[5] H. Kim, J. Jung, W. Lee, S. Nam, and J. Oh, "D-band 4 × 4 multi-feed array antenna-in-package for high-power combining and polarization synthesis," *IEEE Access*, vol. 11, pp. 144006–144016, 2023.

[6] A. Altaf and M. Seo, "SIW based D-band single and 2 × 2 MIMO elliptically tapered slot antenna," *IEEE Access*, vol. 11, pp. 87270–87278, 2023.

[7] M. Jaber, M. A. Imran, R. Tafazolli, and A. Tukmanov, "5G backhaul challenges and emerging research directions: A survey," *IEEE Access*, vol. 4, pp. 1743–1766, 2016.

[8] N. Deferm and P. Reynaert, "A 120 GHz fully integrated 10 Gb/s short-range star-QAM wireless transmitter with on-chip bondwire antenna in 45 nm low power CMOS," *IEEE J. Solid-State Circuits*, vol. 49, no. 7, pp. 1606–1616, Jul. 2014.

[9] M. Köhler, J. Hasch, H. L. Blöcher, and L.-P. Schmidt, "Feasibility of automotive radar at frequencies beyond 100 GHz," *Int. J. Microw. Wireless Technol.*, vol. 5, no. 1, pp. 49–54, Feb. 2013.

[10] T. Li, A. Bhutani, and T. Zwick, "A D-band corporate-feed gap-cavity slot array antenna using virtual PEC method," *IEEE Trans. Antennas Propag.*, vol. 70, no. 8, pp. 7258–7263, Aug. 2022.

[11] Z.-W. Miao, Z.-C. Hao, G. Q. Luo, L. Gao, J. Wang, X. Wang, and W. Hong, "140 GHz high-gain LTCC-integrated transmit-array antenna using a wideband SIW aperture-coupling phase delay structure," *IEEE Trans. Antennas Propag.*, vol. 66, no. 1, pp. 182–190, Jan. 2018.

[12] A. Altaf, W. Abbas, and M. Seo, "A wideband SIW-based slot antenna for D-band applications," *IEEE Antennas Wireless Propag. Lett.*, vol. 20, pp. 1868–1872, 2021.

[13] H. H. Bae, T. H. Jang, H. Y. Kim, and C. S. Park, "Broadband 120 GHz L-probe differential feed dual-polarized patch antenna with soft surface," *IEEE Trans. Antennas Propag.*, vol. 69, no. 10, pp. 6185–6195, Oct. 2021.

[14] A. Bisognin, N. Nachabe, C. Luxey, F. Gianesello, D. Gloria, J. R. Costa, C. A. Fernandes, Y. Alvarez, A. Arboleya-Arboleya, J. Laviada, F. Las-Heras, N. Dolatsha, B. Grave, M. Sawaby, and A. Arbabian, "Ball grid array module with integrated shaped lens for 5G backhaul/fronthaul communications in F-band," *IEEE Trans. Antennas Propag.*, vol. 65, no. 12, pp. 6380–6394, Dec. 2017.

[15] Q.-Y. Guo and H. Wong, "155 GHz dual-polarized Fabry–Pérot cavity antenna using LTCC-based feeding source and phase-shifting surface," *IEEE Trans. Antennas Propag.*, vol. 69, no. 4, pp. 2347–2352, Apr. 2021.

[16] P. Wang, J. Liu, C. Zhou, B. Yin, and W. Wang, "Dual-band dual-circularly polarized Fabry–Pérot cavity MIMO antenna using CMM-based polarization converter and MMA for vehicular satellite communications," *IEEE Trans. Veh. Technol.*, pp. 1–12, 2023.

[17] A. Hosseini, S. Kabiri, and F. De Flaviis, "*V*-band high-gain printed quasi-parabolic reflector antenna with beam-steering," *IEEE Trans. Antennas Propag.*, vol. 65, no. 4, pp. 1589–1598, Apr. 2017.

[18] Y. Guo, Y. Li, J. Wang, L. Ge, Z. Zhang, M. Chen, Z. Li, B. Ai, and R. He, "A 3D printed nearly isotropic Luneburg lens antenna for millimeter-wave vehicular networks," *IEEE Trans. Veh. Technol.*, vol. 71, no. 2, pp. 1145–1155, Feb. 2022.

[19] G. H. Elzwawi, A. Kesavan, R. Alwahishi, and T. A. Denidni, "A new corner-reflector antenna with tunable gain based on active frequency selective surfaces," *IEEE Open J. Antennas Propag.*, vol. 1, pp. 88–94, 2020.

[20] A. E. Bezer, M. Abbak, T. Gursoy, and U. Aydin, "Comparison of 122 GHz lens antennas for system-on-chip FMCW radar with minimum back reflection and high gain," *IEEE Antennas Wireless Propag. Lett.*, vol. 19, pp. 2329–2333, 2020.

[21] N. T. Nguyen, A. V. Boriskin, L. Le Coq, and R. Sauleau, "Improvement of the scanning performance of the extended hemispherical integrated lens antenna using a double lens focusing system," *IEEE Trans. Antennas Propag.*, vol. 64, no. 8, pp. 3698–3702, Aug. 2016.

[22] M. Alonso-delPino, C. Jung-Kubiak, T. Reck, N. Llombart, and G. Chattopadhyay, "Beam scanning of silicon lens antennas using integrated piezomotors at submillimeter wavelengths," *IEEE Trans. Terahertz Sci. Technol.*, vol. 9, no. 1, pp. 47–54, Jan. 2019.

[23] A. E. I. Lamminen, S. K. Karki, A. Karttunen, M. Kaunisto, J. Säily, M. Lahdes, J. Ala-Laurinaho, and V. Viikari, "Beam-switching dual-spherical lens antenna with low scan loss at 71–76 GHz," *IEEE Antennas Wireless Propag. Lett.*, vol. 17, pp. 1871–1875, 2018.

[24] K. Liu, S. Yang, S.-W. Qu, C. Chen, and Y. Chen, "Phased hemispherical lens antenna for 1-D wide-angle beam scanning," *IEEE Trans. Antennas Propag.*, vol. 67, no. 12, pp. 7617–7621, Dec. 2019.

[25] M. A. Campo, G. Carluccio, S. Bruni, and N. Llombart, "Dielectric gratings enhancing the field of view in low dielectric permittivity elliptical lenses," *IEEE Trans. Antennas Propag.*, vol. 69, no. 11, pp. 7308–7322, Nov. 2021.

[26] S. van Berkel, E. S. Malotaux, C. De Martino, M. Spirito, D. Cavallo, A. Neto, and N. Llombart, "Wideband double leaky slot lens antennas in CMOS technology at submillimeter wavelengths," *IEEE Trans. THz Sci. Technol.*, vol. 10, no. 5, pp. 540–553, Sep. 2020.

[27] K. Konstantinidis, A. P. Feresidis, C. C. Constantinou, E. Hoare, M. Gashinova, M. J. Lancaster, and P. Gardner, "Low-THz dielectric lens antenna with integrated waveguide feed," *IEEE Trans. THz Sci. Technol.*, vol. 7, no. 5, pp. 572–581, Sep. 2017.

[28] N. Chudpooti, P. Sangpet, T. Pechrkool, N. Duangrit, W. Thaiwirot, P. Akkaraekthalin, and N. Somjit, "An additive 3D-printed hemispherical lens with flower-shaped stub slot ultra-wideband antenna for high-gain radiation," *IEEE Access*, vol. 11, pp. 91225–91233, 2023.

[29] N. Ghassemi and K. Wu, "Millimeter-wave integrated pyramidal horn antenna made of multilayer printed circuit board (PCB) process," *IEEE Trans. Antennas Propag.*, vol. 60, no. 9, pp. 4432–4435, Sep. 2012.

[30] J. Hu, Y. Li, S. Wang, and Z. Zhang, "Millimeter-wave air-filled slot antenna with conical beam based on bulk silicon MEMS technology," *IEEE Trans. Antennas Propag.*, vol. 68, no. 5, pp. 4077–4081, May 2020.

[31] S. M. Sifat, S. I. Shams, and A. A. Kishk, "Ka-band integrated multilayer pyramidal horn antenna excited by substrate-integrated gap waveguide," *IEEE Trans. Antennas Propag.*, vol. 70, no. 6, pp. 4842–4847, Jun. 2022.

[32] B. Cao, H. Wang, Y. Huang, J. Wang, and H. Xu, "A novel antenna-in-package with LTCC technology for W-band application," *IEEE Antennas Wireless Propag. Lett.*, vol. 13, pp. 357–360, 2014.

[33] C. Ma, S. Ma, L. Dai, Q. Zhang, H. Wang, and H. Yu, "Wideband and high-gain D-band antennas for next-generation short-distance wireless communication chips," *IEEE Trans. Antennas Propag.*, vol. 69, no. 7, pp. 3700–3708, Jul. 2021.

[34] D. A. Montofré, R. Molina, A. Khudchenko, R. Hesper, A. M. Baryshev, N. Reyes, and F. P. Mena, "High-performance smooth-walled horn antennas for THz frequency range: Design and evaluation," *IEEE Trans. THz Sci. Technol.*, vol. 9, no. 6, pp. 587–597, Nov. 2019.

[35] T. J. Douglas, A. Y. Nashashibi, H. N. Shaman, and K. Sarabandi, "Sub-millimeter-wave polarization-independent spatial power divider for a two-port dual-polarized antenna," *IEEE Trans. THz Sci. Technol.*, vol. 11, no. 5, pp. 508–518, Sep. 2021.

[36] D. Caratelli, R. Cicchetti, V. Cicchetti, and O. Testa, "A wideband high-gain circularly-polarized dielectric horn antenna equipped with Lamé-axicon stacked-disk lens for remote sensing, air traffic control and satellite communications," *IEEE Access*, vol. 11, pp. 20912–20922, 2023.
[37] F. Ahmed, M. U. Afzal, T. Hayat, K. P. Esselle, and D. N. Thalakotuna, "Self-sustained rigid fully metallic metasurfaces to enhance gain of shortened horn antennas," *IEEE Access*, vol. 10, pp. 79644–79654, 2022.
[38] J. Lorente-López, J.-V. Rodríguez, F. Quesada-Pereira, L. Juan-Llácer, and I. Rodríguez-Rodríguez, "UTD-PO solution for E-plane radiation pattern calculation of rectangular horn antennas with rectangular-shaped corrugations," *IEEE Access*, vol. 11, pp. 17424–17429, 2023.
[39] F. Oktafiani, E. Y. Hamid, and A. Munir, "Wideband dual-polarized 3D printed quad-ridged horn antenna," *IEEE Access*, vol. 10, pp. 8036–8048, 2022.
[40] N. Lee, C. Im, S. Park, and H. Choo, "Design of a metal 3D printed double-ridged horn antenna with stable gain and symmetric radiation pattern over a wide frequency range," *IEEE Access*, vol. 11, pp. 100565–100572, 2023.
[41] K. Debbarma, N. Truong, S. K. Sharma, and J. S. Chieh, "2-D beam steering performance of a triple mode horn antenna integrated with Risley prism and phase correcting surface," *IEEE Open J. Antennas Propag.*, vol. 3, pp. 752–761, 2022.
[42] I. Goode and C. E. Saavedra, "3-D printed dually symmetric orthomode transducer and horn antenna at X-band," *IEEE Open J. Antennas Propag.*, vol. 4, pp. 383–391, 2023.
[43] I. Goode and C. E. Saavedra, "3D printed linearly polarized X-band conical horn antenna and lens," *IEEE Open J. Antennas Propag.*, vol. 3, pp. 549–556, 2022.
[44] S. Diana, D. Brizi, C. Ciampalini, G. Nenna, and A. Monorchio, "A compact double-ridged horn antenna for ultra-wide band microwave imaging," *IEEE Open J. Antennas Propag.*, vol. 2, pp. 738–745, 2021.

MING-AN CHUNG (Senior Member, IEEE) received the B.Eng. and M.Eng. degrees in electronic engineering from Chang Gung University, Taoyuan, Taiwan, in 2003 and 2005, respectively, and the D.Eng. degree in electrical engineering from the National Taiwan University of Science and Technology (NTUST), Taipei, Taiwan, in 2016. He is currently an Associate Professor with the Department of Electronic Engineering, National Taipei University of Technology (NTUT), where is also the Leader of the Innovation Wireless Communication and Electromagnetic Applications Laboratory. His research interests include wireless communication propagation, intelligent robotics, self-driving vehicles, antenna design for various mobile and wireless communications, electromagnetic theory, and applications. He is a Reviewer of many scientific journals, including IEEE TRANSACTIONS ON ANTENNAS AND PROPAGATION, IEEE TRANSACTIONS ON INDUSTRIAL INFORMATICS, *Journal of Intelligent & Robotic Systems*, *IET Microwaves, Antennas and Propagation*, IEEE ANTENNAS AND WIRELESS PROPAGATION LETTERS, *International Review of Electrical Engineering*, *International Journal on Communications Antenna and Propagation*, *AEÜ-International Journal of Electronics and Communications*, and many international conferences, including ICRA, ICCE-TW, RFIT, ICBEB, EMCAR, and SNSP.

CHIA-WEI LIN received the B.S. and M.S. degrees from Chung Yuan Christian University, in 2007. He is currently pursuing the Ph.D. degree in electrical engineering with the National Taipei University of Technology. His research interests include wireless communication propagation research, antenna design, intelligent robotics research, self-driving vehicle research, embedded systems, and deep learning.

ING-PENG MEIY received the master's degree in electronic engineering from the National Taipei University of Technology, in 2023. His current research interests include millimeter-wave and sub-terahertz antenna research, chip filter research, and other RFIC component research.